Thermoelectric Infrared Imaging Sensors for Automotive Applications

Hirota, Masaki
Nissan Motor Co., Ltd. (Japan)

Nakajima, Yasushi
Nissan Motor Co., Ltd. (Japan)

Saito, Masanori
Nissan Motor Co., Ltd. (Japan)

Satou, Fuminori
Nissan Motor Co., Ltd. (Japan)

他

Thermoelectric Infrared Imaging Sensors
for Automotive Applications

Masaki Hirota[*a], Yasushi Nakajima[a], Masanori Saito[b], Fuminori Satou[a] and Makoto Uchiyama[a]

[a]Electronics and Information Technology Research Laboratory,
[b]Testing and Technical Service Department,
Nissan Research Center, Nissan Motor Co., Ltd.
1 Natsushima-cho, Yokosuka 237-8523, Japan

ABSTRACT

This paper describes three low-cost thermoelectric infrared imaging sensors having a 1,536, 2,304, and 10,800 element thermoelectric focal plane array (FPA) respectively and two experimental automotive application systems. The FPAs are basically fabricated with a conventional IC process and micromachining technologies and have a low cost potential. Among these sensors, the sensor having 2,304 elements provide high responsivity of 5,500 V/W and a very small size with adopting a vacuum-sealed package integrated with a wide-angle ZnS lens. One experimental system incorporated in the Nissan ASV-2 is a blind spot pedestrian warning system that employs four infrared imaging sensors. This system helps alert the driver to the presence of a pedestrian in a blind spot by detecting the infrared radiation emitted from the person's body. The system can also prevent the vehicle from moving in the direction of the pedestrian. The other is a rearview camera system with an infrared detection function. This system consists of a visible camera and infrared sensors, and it helps alert the driver to the presence of a pedestrian in a rear blind spot. Various issues that will need to be addressed in order to expand the automotive applications of IR imaging sensors in the future are also summarized. This performance is suitable for consumer electronics as well as automotive applications.

Keywords: Infrared, sensors, thermoelectric, thermopiles, automotive, vehicles, blind spot, and Au Black

1.INTRODUCTION

It is said that drivers generally obtain the greater part of the information needed for driving through their faculty of vision. In recent years, a great deal of research and development work has been done on systems that use infrared (IR) radiation primarily to assist drivers' outward view. Infrared radiation refers to light having wavelengths (0.7 μm-1.0 mm) longer than those of visible light (0.38-0.7μm) perceptible to the human eye. There are three atmospheric transmittance regions of IR radiation: short-wavelength IR (SWIR, 0.7-2 μm), mid-wavelength IR (MWIR, 3-5 μm) and long-wavelength IR (LWIR, 8-13 μm). Among these three regions, the human body and various other types of warm bodies near room temperature naturally radiate LWIR light. This means that LWIR technology can be employed to detect the human body even at night without using any illumination. However, the energy level of LWIR light is very low compared with that of visible light. Hence, some resourcefulness is required to detect LWIR light, such as by cooling the detector to an ultra-low temperature or by first converting IR energy to thermal energy.

Development work aimed at applying LWIR technology to automobiles began in the 1980s, but full-fledged application efforts were not initiated until after it was demonstrated that two types of uncooled IR imaging sensors could provide performance nearly comparable to that of cooled devices. That occurred in 1992, when Texas Instruments [1] and Honeywell [2] took uncooled IR sensors that had originally been developed for military use and implemented them in commercial applications. In 1999, a system [3] was put on the market that uses that sensor technology to provide IR images of the road ahead to drivers at night.

Many research institutes have been actively engaged in the development of IR sensors since the early 1990s. To date, various types of uncooled IR imaging sensors have been developed, including the thermoelectric type, [4-7] the amorphous silicon bolometer [8] and the silicon-on-insulator (SOI) diode. [9] Meanwhile, systems using SWIR

technology to provide IR images have also begun to be commercialized. Such systems are expected to undergo further development in the coming years on account of their various advantages. Because SWIR sensors share many aspects in common with visible light sensor technologies, the devices can be obtained at relatively low cost. Moreover, SWIR images are easy for drivers to understand because their contrast is close to that of visible light images.

At Nissan, we conducted fundamental studies of IR sensor technologies during the 1980s, and subsequently took part in the Advanced Safety Vehicle (ASV) project that the Ministry of Transport (currently the Ministry of Land, Infrastructure and Transport) initiated in 1991. On the basis of that research, we have proposed the world's first nighttime pedestrian warning system [10] that uses uncooled LWIR cameras to detect pedestrians and first blind spot pedestrian warning system that incorporates a brake control capability to prevent the host vehicle from starting off in the direction of a detected human body. The application of uncooled IR imaging sensors, however, is still limited to luxury cars at present because of the high device cost. Infrared imaging sensors must be further reduced in cost in order to promote their widespread use in automotive systems, such as those for helping drivers to see objects in blind spots or for detecting the presence of vehicle occupants.

Various types of uncooled IR imaging sensors have already been proposed. However, in order to obtain ultra-high sensitivity, most of them adopt exceptionally complex structures or employ materials that are not compatible with the conventional IC manufacturing process, making it difficult to reduce their cost. Among these various sensor types, we have focused on the thermoelectric IR imaging sensor because of its low cost potential, stemming from its high compatibility with the conventional IC production process, absence of any need for a temperature control mechanism or an optical chopper, and design ease of the second-stage processing circuit owing to the device's thermoelectric nature. A CCD type of thermoelectric IR imaging sensor with over 10,000 elements has already been announced, but we have adopted a CMOS imager system with the aim of reducing the device cost further. High sensor performance has been achieved as a result of further miniaturizing and optimizing our thermoelectric IR imaging sensors.

This paper gives an overview of thermoelectric IR sensor systems for automotive applications, describes the status of the IR imaging sensors now under development in our laboratories, and explains the blind spot pedestrian warning system incorporated in the Nissan ASV as well as a rearview camera system with an IR detection function.
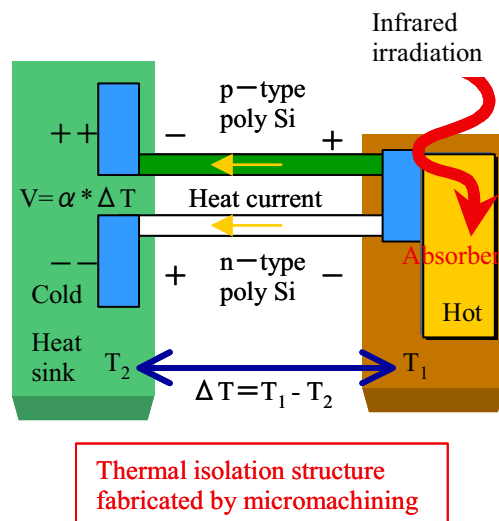
Fig. 1. Operating principle of a thermoelectric IR sensor

2. THERMOELECTRIC IR SENSORS

2.1. Operating principle and features
A thermoelectric IR sensor (thermopile) detects the intensity of incident IR radiation by using tiny thermocouples to convert the temperature rise of a Au-black absorber, resulting from IR absorption, to a voltage signal (Fig. 1). To

increase the absorptivity of incident IR radiation, we have developed a Au-black absorber that achieves high IR absorptivity of more than 90% (Fig 2). The Au-black absorber is patterned precisely in a lift-off process using a PSG sacrificial layer. The formation accuracy of this process, developed independently in our laboratories, is 1,000 times greater than that of conventional partial evaporation deposition and the dripping method. This makes it possible to form the Au-black absorber, which has been difficult to pattern precisely, with the same patterning accuracy as that of the conventional CMOS IC process. In addition, the Au-black absorber is formed on a thin membrane, fabricated by micromachining to a thickness of less than 2 μm, and is thermally insulated by sealing the surrounding area under a high vacuum of less than 1×10^{-1} Pa, thereby increasing the temperature rise of the absorber. One distinctive feature of this thermoelectric IR sensor is its simplified latter stage circuitry, owing to the fact that it can detect IR radiation without the passage of a bias current, unlike a bolometer and other sensors. The thermocouples are fabricated of p-type and n-type polysilicon, which allows the use of low-cost ultra-fine microfabrication technology commonly employed in the conventional semiconductor manufacturing process, and thermocouple pairs are connected in series to enhance responsivity.

(a) Tilted 45 deg.

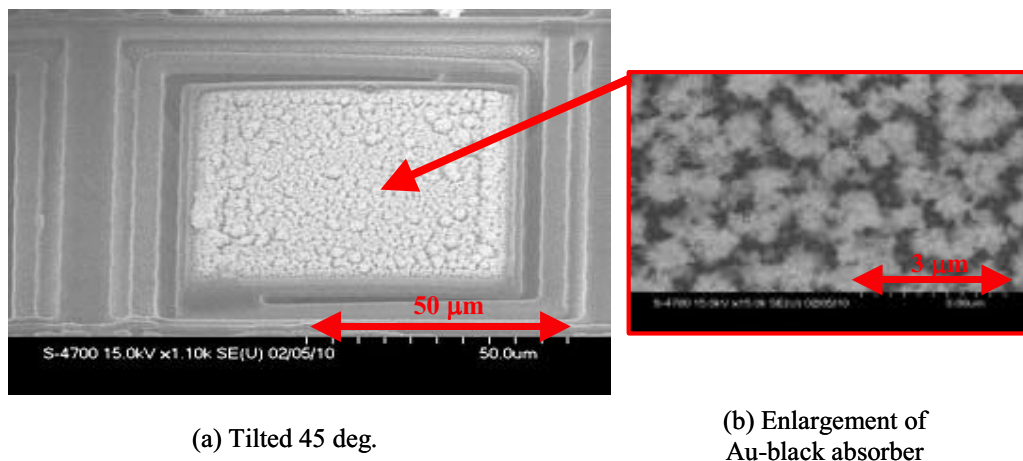(b) Enlargement of
Au-black absorber

Fig. 2. SEM micrographs of (a) one element of a thermopile and (b) Au-black absorber

2.2. Overview of sensor fabrication process

The sequence of operations in the fabrication process of this thermoelectric IR sensor is shown in Fig. 3. The sensor is produced in a process involving the formation of two metal layers, two polysilicon layers, a 0.8-μm CMOS process and seven special operations.

First, the transistors and other devices are fabricated on a p-type (100) Si substrate in an ordinary CMOS process (step a). This ordinary CMOS process also includes thermopile fabrication and formation of the SiN film that serves as the thin membrane. As mentioned above, the thermopiles are fabricated from p-type and n-type polysilicon. The p-type polysilicon is doped with a boron dose of 1×10^{16} cm^{-2} and the n-type silicon is doped with a phosphorous dose of 1×10^{16} cm^{-2}. Next, a phosphous silicate glass (PSG) sacrificial layer is deposited (step b), and then the thermal isolation structure is fabricated by immersing the wafer in hydrazine at 80°C for 75 min. to remove part of the Si substrate (step c). That is followed by formation of the Au-black absorber in a low-pressure vacuum evaporation process (step d). This process is performed by first evacuating the chamber to a pressure of 1×10^{-2} Pa and then introducing N$_2$ gas to an elevated pressure of 2.66×10^2 Pa, after which gold is heated in the boat and evaporated under that condition. Because the mean free path of the gas species is very short at that pressure, three-dimensional growth is dominant, and the surface of the deposited Au-black layer becomes like cotton. The thickness of the deposited layer is approximately 3.0 μm. This process reduces the surface reflectivity of the deposited layer, making it possible to obtain exceptionally high IR absorptivity of more than 90% at wavelengths of 8-13 μm. Finally, the Au-black layer is patterned in a lift-off process in which the unwanted PSG sacrificial layer is removed with a pad etchant (step e). Since the density of Au-black is only about 1/20 of that of the deposited thin Au layer, the pad etchant easily penetrates the Au-black layer to complete the lift-off process in a short time of about 4 min.
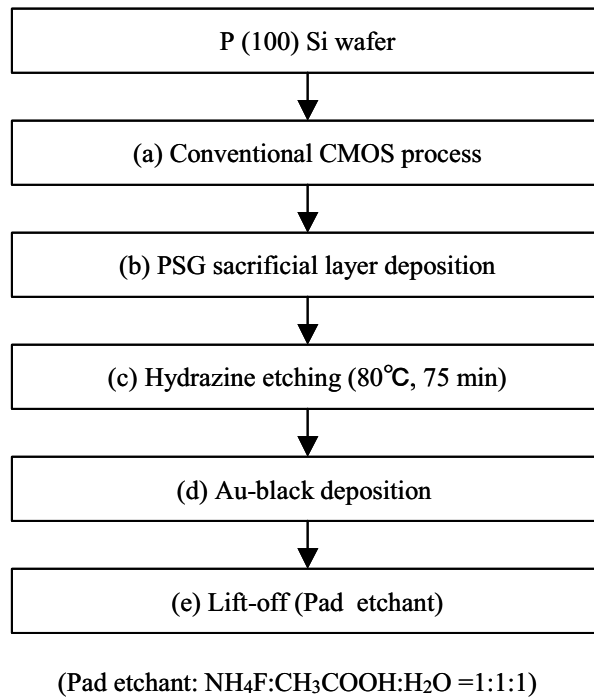
```
┌─────────────────────────────────────────┐
│            P (100) Si wafer              │
└─────────────────────────────────────────┘
                    │
                    ▼
┌─────────────────────────────────────────┐
│        (a) Conventional CMOS process     │
└─────────────────────────────────────────┘
                    │
                    ▼
┌─────────────────────────────────────────┐
│      (b) PSG sacrificial layer deposition │
└─────────────────────────────────────────┘
                    │
                    ▼
┌─────────────────────────────────────────┐
│      (c) Hydrazine etching (80℃, 75 min) │
└─────────────────────────────────────────┘
                    │
                    ▼
┌─────────────────────────────────────────┐
│          (d) Au-black deposition         │
└─────────────────────────────────────────┘
                    │
                    ▼
┌─────────────────────────────────────────┐
│         (e) Lift-off (Pad  etchant)      │
└─────────────────────────────────────────┘
```

(Pad etchant: $NH_4F:CH_3COOH:H_2O =1:1:1$)

Fig. 3. Sensor fabrication process

2.3. Prediction of sensor performance

This section describes the calculations that were done to optimize the sensor parameters in order to achieve both high responsivity and fast response. The responsivity (R) of a thermopile is given by

$$R = n \bullet \alpha \bullet R_{th} \bullet \eta \qquad (1)$$

where R is responsivity, n is the number of thermopile pairs, α is the Seebeck coefficient (sum of the p-type and n-type polysilicon), R_{th} is the thermal resistance between the hot and cold junctions, and η is incident IR radiation absorptivity. In general, it is presumed that the number of thermopile pairs, n, has to be increased in order to improve thermopile responsivity. Increasing n, however, must be carefully examined in detail because it causes thermal resistance, R_{th}, to decline. As shown in Table 1, in atmospheric-pressure sealed thermopiles, which are the most numerous device on the market, the thermal resistance, R_{th}, between the hot and cold junctions equals the parallel connection between the thermal resistance of the membrane, $R_{th(membrane)}$, and the thermal resistance of the charged gas, $R_{th(gas)}$. In this case, the responsivity improvement is limited because the maximum value of R_{th} cannot exceed $R_{th(gas)}$ even if $R_{th(membrane)}$ is increased. Accordingly, improving the responsivity of atmospheric-pressure sealed thermopiles requires an increase in the number of pairs, n, rather than in R_{th}. Increasing n, however, produces greater electrical resistance, R_{ele}, in the thermopile, resulting in higher Johnson noise (thermal noise). On the other hand, in the case of vacuum-sealed sensors like the one described here, the thermal resistance of the charged gas, $R_{th(gas)}$, is extremely large, and the thermal resistance, R_{th}, between the hot and cold junctions is determined by the thermal resistance of the membrane, $R_{th(membrane)}$. By using beams with a large $R_{th(membrane)}$, high responsivity can be obtained even with a small number of thermopile pairs, n. In this case, the electrical resistance of the thermopile, R_{ele}, is reduced, and a high signal-to-noise (S/N) ratio can be obtained without increasing Johnson noise. The dependence of responsivity, R, on the number of pairs, n, was calculated for an element size of 100 x 100 μm, a thermopile width of 0.8 μm, a thermopile pitch of 1.6 μm and an etch hole width of 2.4 μm, and n was optimized on that basis. The Seebeck coefficient was set at 0.49 mV/K for one thermopile pair. As shown in Fig. 4, responsivity initially increases with an increasing number of thermopile pairs, n, but it reaches nearly its maximum value at n = 2-4. Any further increase in n has the effect of reducing responsivity because the reduced area of the absorber layer becomes predominant. Based on these results, we set the number of pairs at n = 2 because a condition of n = 2-4 allows a low level of electrical resistance and a reduction of thermal noise. Responsivity of 3,900 V/W and electrical resistance of 90 kΩ were calculated at n = 2.
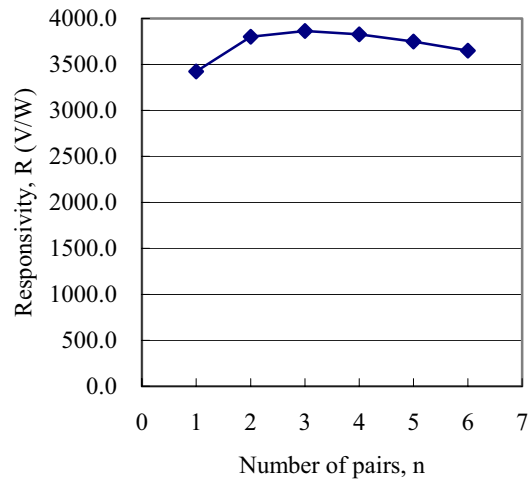
Fig. 4. Responsivity as a function of the number of thermopile pairs (simulation)

2.4. 2-D focal plane array (FPA)

To date, we have developed three types of IR imaging sensors. The features of each sensor are shown in Fig. 5 and their specifications are listed in Table 2.
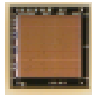
	Type 1	Type 2	Type 3
FPA			
Element			
Packaged sensor			
Image			

Fig. 5. Three types of IR imaging sensors developed to date

The type 1 sensor is the first-generation device developed in 1998 with 48 x 32 elements and an element pitch of 190 µm. The IR radiation absorber of this sensor is supported by four beams in a gammadion-shaped structure, as indicated in Fig. 5. The dimensions of the various parts of the sensor are as follows: chip size of 10.5 x 7.44 mm, element pitch of

190 x 190 μm, Au-black absorber size of 116 x 116 μm, six pairs of thermopiles, beam width of 14 μm and thermopile width of 0.8 μm. The output terminal of each element is connected to an output line through two built-in NMOS transistors controlled by an external input signal. The negative terminal of all the elements is connected to the same common terminal. Additionally, because this sensor has comparatively high internal resistance of 116 kΩ, it is necessary to limit the bandwidth of the second-stage circuit for the purpose of reducing Johnson noise. In order to obtain the desired video frame rate, the entire sensor is divided into 12 blocks of four columns each, and signals are output in parallel from 12 output lines. In the vacuum-sealed package (Fig. 5), this sensor achieves responsivity of R = 2,100 V/W and a thermal time constant of τ = 25 msec, representing high levels of performance compared with similar commercial devices. This IR imaging sensor is used in all the automotive application systems that will be described later.

The type 2 sensor is the second-generation device with 120 x 90 elements and was developed with the objectives of increasing resolution, extending the detection distance and expanding the field of view. For the purpose of increasing resolution, the element pitch was reduced by 48% from 190 μm to 100 μm. As a result, the area occupied by the elements, i.e., the amount of incident IR energy, was reduced to approximately one-fourth. The output signal level was maintained by increasing the thermal resistance between the hot and cold junctions and increasing the fill factor numerical aperture. The beam width of this sensor was reduced to less than one-third of the previous width (from 14 μm to 4.4 μm), and an L-shaped structure with two beams was adopted to support the IR radiation absorber, which substantially improved thermal resistance. The dimensions of the various parts of the sensor are as follows: chip size of 14.4 x 11.0 mm, element size of 100 x 100 μm, Au-black absorber size of 65 x 65 μm, two pairs of thermopiles, beam width of 4.4 μm and thermopile width of 0.8 μm. Like the 48 x 32 element sensor, this sensor is also divided into 12 blocks in order to reduce the noise level. As a result of the improvements made to the various components, this second-generation sensor achieves responsivity of R = 3,900 V/W, a further improvement in performance over the previous device.

Table 2. Specifications of three types of IR imaging sensors

Array Property	Type 1	Type 2	Type 3
Array size (elements)	48 x 32	120 x 90	48 x 48
Element pitch (μm)	190	100	100
Fill factor (%)	37	42	52
Thermopile pairs	6	2	2
Thermopile width (μm)	0.8	0.8	0.34
Numbers of beams	4	2	2
Beam width (μm)	14	4.4	3.1
Responsivity (V/W)	2,100	3,900	5,500
Time constant (msec)	25	44	53
Resistance (kΩ)	116	90	230
Die size (mm)	9.0 x 7.44	14 x 11	6.5 x 6.5
Window	Ge	Ge	ZnS lens
Field of view (deg)	-	-	100
Package size (mm in diameter)	44	44	15

The type 3 sensor is the third-generation device with 48 x 48 elements and was developed with the aims of achieving even higher responsivity and a smaller size. Further size and cost reductions were achieved by adopting a vacuum-sealed package integrated with a wide-angle ZnS lens (Fig. 5). The element pitch is 100 μm, the same as that of the type 2 device, but the thermopile width has been reduced by two-thirds from 0.8 μm to 0.34 μm, and the beam width has also been reduced by about 30% from the previous dimension of 4.4 μm to 3.1 μm. These changes have further improved thermal resistance, and the type 3 sensor achieves responsivity of R = 5,500 V/W. The chip size is 6.5 x 6.5 mm, including a built-in scanning circuit. Additionally, the window material of the TO-8 vacuum-sealed package was fabricated as a lens having a focal length of f = 2 mm and an 80° field of view, thereby making an additional lens

unnecessary. The compactness of this sensor is especially advantageous for use in systems installed in the passenger compartment.

2.5. High-speed response

Efforts have also been made to improve the response speed, which is another issue of thermoelectric IR sensors. Previously, thermoelectric IR sensors had such problems as low responsivity and slow response, compared with quantum devices, though they could be used without any cooling. As a result of optimizing the device structure on the basis of simulations conducted with a thermal equivalent circuit, we have succeeded in developing a sensor that achieves a thermal time constant of $\tau_e = 270$ μsec and responsivity of R = 60 V/W.

In general, the response speed of thermopiles is limited by the thermal time constant, τ_{th}, which is proportional to the thermal resistance, R_{th}, and thermal capacity, C_{th}, as seen in the following equation.

$$\tau_{th} \propto C_{th} \cdot R_{th} \tag{2}$$

Accordingly, it is necessary to reduce the thermal capacity, C_{th}, without changing the thermal resistance, R_{th}, in order to improve the response speed without sacrificing responsivity. Thermal resistance, R_{th}, is equal to the ratio of the distance between the hot and cold junctions to the cross-sectional area. Accordingly, by reducing the cross-sectional area of the thermopiles and membrane, the thermal resistance, R_{th}, i.e., responsivity, R, can be maintained even if the thermopile length is shortened. Moreover, shortening the thermopile length reduces the thermal capacity, C_{th}, i.e., the thermal time constant, τ_{th}, making it possible to achieve high-speed operation.

Figure 6 is micrograph of a prototype high-speed sensor, having outer dimensions of 144 x 144 μm. The Au-black absorber measures 112 x 112 μm. Thirty-four pairs of thermopiles, consisting of alternating layers of p-type and n-type polysilicon and connected by a thin Al wiring layer, are formed on a 300-nm-thick SiN membrane. To form the membrane, an anisotropic etching method is used through the etching holes in the surface. Figure 7 shows the response waveform of the high-speed sensor. The thermal time constant was approximated with a first-order delay system to be τ_e = 270 μsec. This value is approximately one-tenth of that of the previous sensor having the same responsivity. As a result, this prototype sensor achieves high-speed operation that is ten times faster than the previous device.
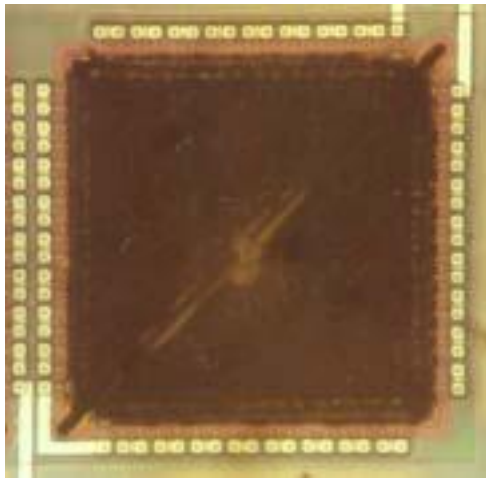

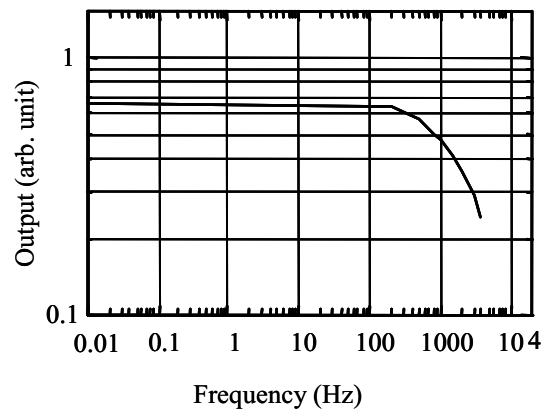Fig. 6. SEM micrograph of high-speed sensor

Fig. 7. Frequency response of high-speed sensor

3. RESEARCH ON AUTOMOTIVE IR SYSTEMS

3.1. Classification of IR sensor application systems

Far-infrared (FIR) sensors are promising devices for use in various systems as human body detection sensors and noncontact thermometers. Examples of systems for automotive applications and their required performance are given in Table 3.

Table 3. Classification of IR sensor systems for automotive applications

classification	Categories	Examples	Required performance
By benefit	Improving safety	Pedestrian detection, occupant detection	High reliability
	Improving comfort	Cabin climate control, HMI	Low cost, accurate temp.
	Others	Diagnostics, anti-theft	Temp. measurement, high reliability, low power consumption
By use	Acquiring thermal distribution images	Pedestrian detection, occupant detection	Reliable recognition of a human body
	Temp. measurement	Cabin climate control, brake temp. measurement, diagnostics	Accurate temp. measurement, fast response
By installation location	Outside cabin	Bumpers, back door, engine compartment	Weatherability, vibration and shock resistance
	Inside cabin	Instrument panel, ceiling	Compact size, good design

3.1.1. Classification by benefit

This classification consists of three major categories: systems for improving safety, systems for improving occupant comfort and others. Safety systems include both active safety technologies, such as a night vision sensor [11] and a pedestrian detection sensor [12], and passive safety technologies typified by intelligent airbags. Examples of systems for improving occupant comfort and convenience include those for passenger compartment climate control by means of an interior IR thermometer and new human-machine interfaces (HMI). The third category comprises systems for diagnostics, anti-theft and other purposes.

3.1.2. Classification by use

Systems can be classified here into three categories: those that only provide images, those that provide the results of image processing for the purpose of detecting pedestrians or vehicle occupants based on the gradations of the acquired IR images, and those that provide a temperature distribution obtained with a noncontact thermometer (radiation thermometer) for cabin climate control or other purposes. Increasingly more advanced measurement technology is required in the order of the first to the third categories. In many cases, it is sufficient if the position of a human body can be identified from the heat distribution in an image acquired with an IR sensor. However, temperature measurements are required for cabin climate control and other applications.

For applications involving measurement of the temperature of in-vehicle equipment, relative temperature measurements are necessary. Examples here include measurement of the engine compartment temperature or the brake rotor temperature.

3.1.3. Classification by place of installation

The places of IR sensor installation in vehicles can be broadly divided between locations inside and outside the passenger compartment. Requirements for installation inside the passenger compartment include a small sensor size and a design that blends in with the interior trim without causing any unnatural feeling. It has become much more difficult to find available space for installing sensors in the cabin of today's cars because much of the space is already occupied by various types of electronic devices, including information devices, typified by navigation systems, and safety equipment such as airbags. It is also likely that instrument panel designs will change substantially in the years ahead under the impact of further advances in navigation systems and information technology (IT). Care must also be exercised in selecting places for sensor installation because the ambient temperature may be higher than the outside air temperature. The general requirements for installation outside the passenger compartment include sufficient weatherability, resistance to vibration and shock resistance, among other properties. Care must be taken in particular with regard to selection of a suitable window material.

3.2. R&D efforts at Nissan

3.2.1. Development of a vehicle-mounted IR camera

At Nissan, we have independently developed a vehicle-mounted IR camera that incorporates the type 1 sensor described above. A photo of the IR camera designed for pedestrian detection is shown in Fig. 8, and its specifications are given in Table 4. The IR imaging sensor is a compact, lightweight device, measuring only 100 mm in width, 60 mm in height (excluding the bracket) and 80 mm in depth and weighing just 400 g. The sensor has a germanium meniscus single-element lens with a focal distance of f = 15 mm and f/0.7. Both sides of the lens are coated with an anti-reflection coating in the 10-μm wavelength band. The field of view is 30° horizontal x 20° vertical. This IR camera operates under a program stored in a Read Only Memory (ROM) incorporated in the Central Processing Unit (CPU, SH7034). The 2-D array sensor outputs signals successively in parallel from its 12 blocks based on an address signal request from the CPU. The output signals are amplified and then sent to the CPU via an 8-bit analog-to-digital converter (ADC). The CPU first performs offset compensation and responsivity compensation on the signals and then makes a pedestrian detection judgment. A function is also provided for converting IR image data to an NTSC video signal using a video digital-to-analog converter (DAC). This IR camera can output an NTSC video signal as well as a pedestrian detection signal and image data via the RS-232C interface. With its f/0.7 lens, the IR camera achieves a noise equivalent temperature deviation (NETD) of less than 0.4°C.

Fig. 8. Vehicle-mounted IR camera incorporated 48 x 32 element FPA

Table 4. Specifications of vehicle-mounted 48 x 32 element IR camera

Performance parameter	Capability (@ 300K)
Array configuration	48 x 32
Chip dimensions	10.5 mm x 7.44 mm
Pixel size	190 μm
Spectral response	8-13 μm
Responsivity	2,100 V/W
Thermal time constant	25 msec
Lens	f = 15 mm, f/0.7
NETD (@ f/0.7)	0.4°C
Field of view	30° x 20°
Outputs	RS-232C, Detection, NTSC
Power	12 V, 3 W
Overall dimensions	100 mm x 60 mm x 80 mm
Weight	400 g

3.2.2. Blind spot pedestrian warning system

This system was proposed in the second phase (1996-2000) of the ASV project and was incorporated in the Nissan ASV-2 [12]. As shown in Fig. 9, four IR cameras incorporating a 48 x 32 element IR sensor array are mounted at the four corners of the vehicle to detect pedestrians in the driver's blind spots. If a pedestrian is present in the direction in which the vehicle is about to move, the system issues a warning and also prevents the vehicle from starting off in that direction. This is the world's first system to provide control of start-off movement by means of IR cameras on an

experimental vehicle. A schematic diagram of the system configuration is shown in Fig. 10. The system mainly consists of the following components: four IR imaging sensor cameras (Fig. 8) with a built-in capability for making pedestrian detection judgments; a blind spot pedestrian warning control unit that integrates the signals from the IR cameras and sends a signal to the Control Area Network (CAN); a vehicle motion control unit (main C/U or Auto Box) that manages vehicle motions; an integrated human-machine interface (HMI) control unit; a monitor and a voice warning unit; and throttle and brake actuators that prevent the vehicle from starting off. The actual operation of the system is as follows. At the time of vehicle launch, the four IR cameras capture start-off images in response to a request from the main control unit and compare them with baseline images that were taken when the vehicle was stopped. If a specified temperature difference and a large heat source are detected in the detection area, the heat source is regarded as a pedestrian and a detection signal is sent to the main control unit. The main control unit issues an audible warning and displays an indication on the monitor screen to alert the driver. In addition, the main control unit activates the brake and throttle actuators that forcibly prevent the vehicle from starting off.

Human body detection distances were measured under different temperature conditions to verify the operation of the prototype system. In a low temperature range of 10-22°C, the detection distance was 6-8 m, which would cover the major part of the rearward blind spot shown in Fig. 9. On the other hand, the detection distance decreased to 3-3.5 m in a higher temperature range of 24-30°C. Under a condition of a temperature difference between the background temperature (Te) and the surface temperature of a pedestrian (Tt) of $\Delta T = Tt - Te \geq 5°C$ (i.e., the atmospheric (background) temperature is no more than 27°C), the detection distance obtained was equal to or greater than the 3-m specification of the prototype system. Moreover, in tests conducted with the Nissan ASV-2, it was confirmed that the system detected the presence of a human body and prevented the vehicle from moving in that direction. These results revealed that the system can be effective in helping to protect pedestrians in the driver's blind spots.

3.2.3. IR camera-equipped experimental vehicle (IREV)

A new experimental vehicle (IREV) has been built, as shown in Fig. 12, to promote the development of a wide range of application systems for the IR sensors now being developed. This experimental vehicle is equipped with the following five systems: a rearview camera with IR detection (IR-RC), an adaptive front-lighting system with IR detection (IR-AFS), an intrusion alarm system, an occupant detection system using a radiation thermometer and a hand command system, representing a new HMI that can recognize the number of extended fingers. The IR-RC system and the IR-AFS system are described in detail below.

The IR-RC system is a fusion of a visible rearview camera and the above-mentioned vehicle-mounted IR camera, enabling it to alert the driver to the presence of a pedestrian in the rearward blind spot by means of an audible warning and a display screen indication. The system configuration is shown in Fig. 12. The image signal from the visible camera and the signals from two IR imaging sensor cameras are processed by a PC to detect heat sources. An integrated detection result is synthesized by an image processor and shown on a dashboard display screen, as illustrated in Fig. 13. The in-vehicle installation of the system is shown in Fig. 14. The detection area is a trapezoid that measures 1.7 m along the width of the vehicle, 2.7 m on its long side and 2.1 m in distance from the rear of the vehicle, as shown in Fig. 12. If a heat source is detected, the driver is alerted by an audible warning and by displaying a red dot on the display screen at a position corresponding to the center of the detected heat source. Under a condition of $\Delta T = Tt - Te \geq 5°C$, this system is capable of detecting a human body in the entire IR detection area.

The IR-AFS system uses IR cameras to detect pedestrians in front of the vehicle, and alerts the driver to their presence by changing the illumination pattern of the headlights in the direction of a detected human body. As illustrated in Fig. 15, IR cameras on either side of the vehicle operate independently to detect pedestrians within a 30° field of view on the outer side of the vehicle's direction of forward travel. The AFS mechanism swivels an auxiliary headlight bulb in increments of approximately 1° to illuminate the direction of a detected pedestrian. A pedestrian detection distance of approximately 10 m has been obtained at present with a prototype system. It is planned to increase the detection distance in the future by using the type 2 sensor.

Four
IR Cameras

Forward movement only

$\geqq$3m

Four IR
Camera

ASV-2

Pedestrian

Detection area
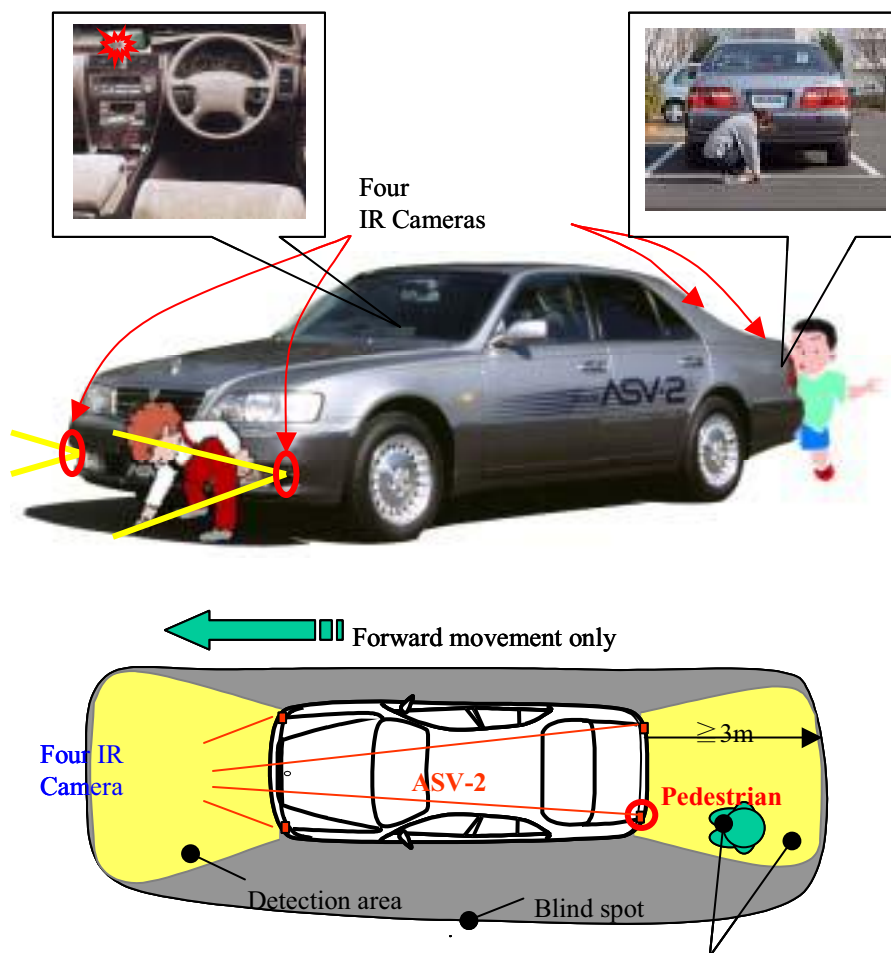
Blind spot

Temperature difference between
the pedestrian and background (ΔT)$\geqq$5℃

Fig. 9. Concept of the blind spot pedestrian warning system

Main C/U (Auto Box)

IR camera

IR camera

Vehicle
information

Voice warning

Throttle
actuator

Monitor

Brake
actuator

CAN

Integrated MHI C/U

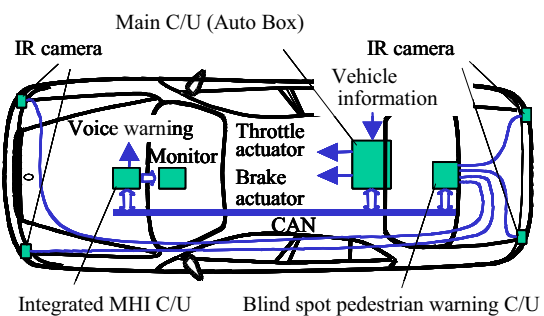Blind spot pedestrian warning C/U

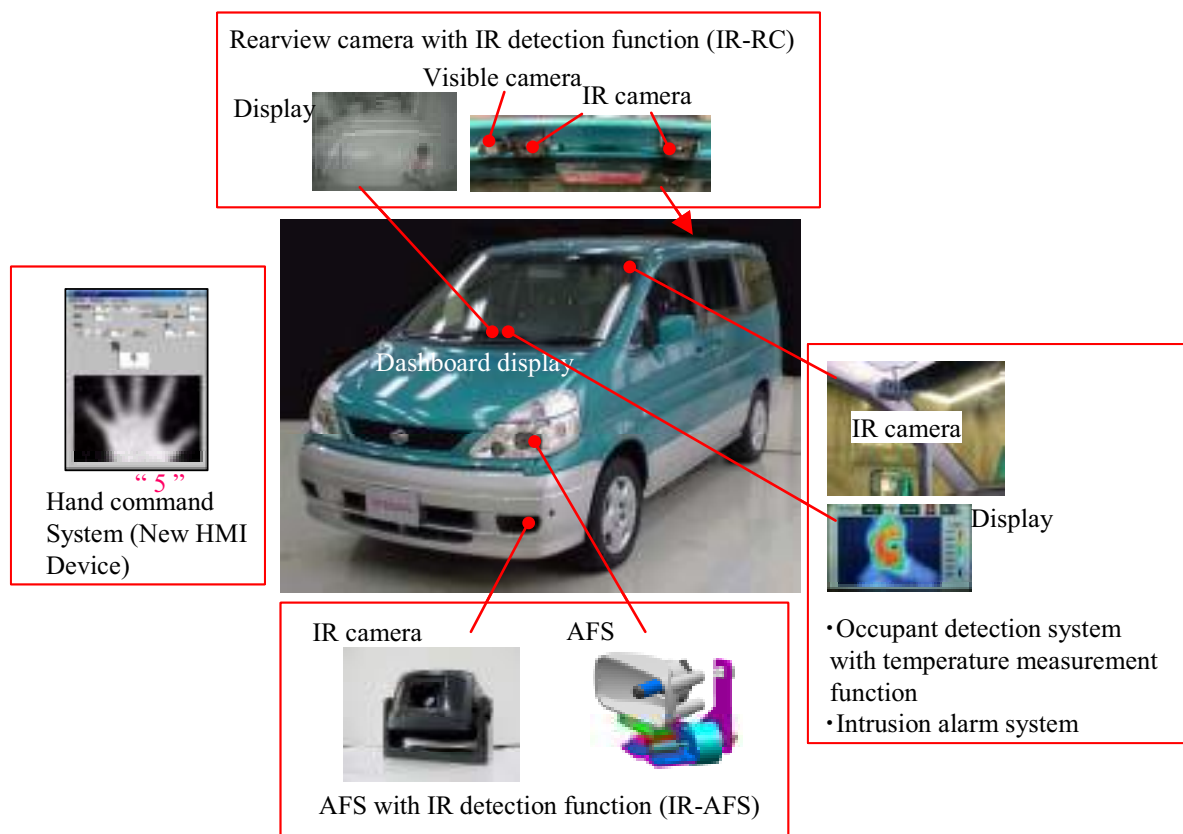Fig. 10. In-vehicle configuration of the blind spot pedestrian warning system

Fig. 11. Experimental vehicle equipped with various IR application systems (IREV)
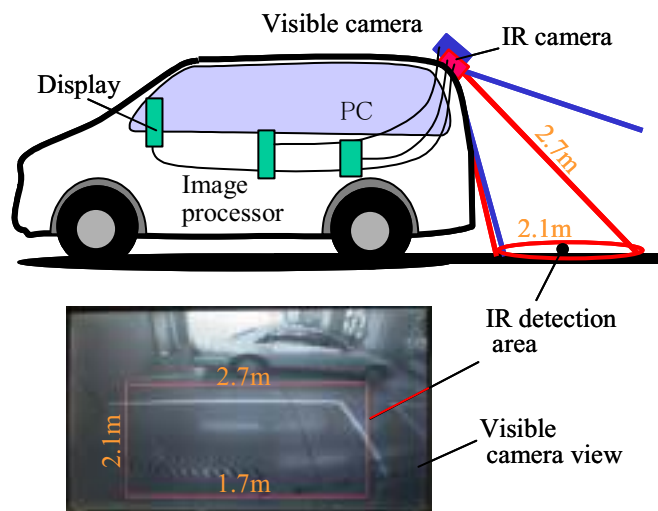

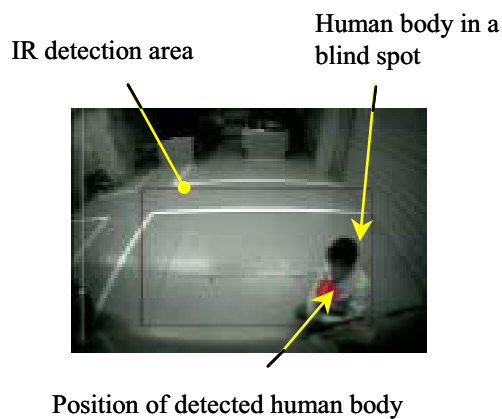Fig. 12. Conceptual diagram of IR-RC system

Fig. 13. Human body detection and display by IR-RC system

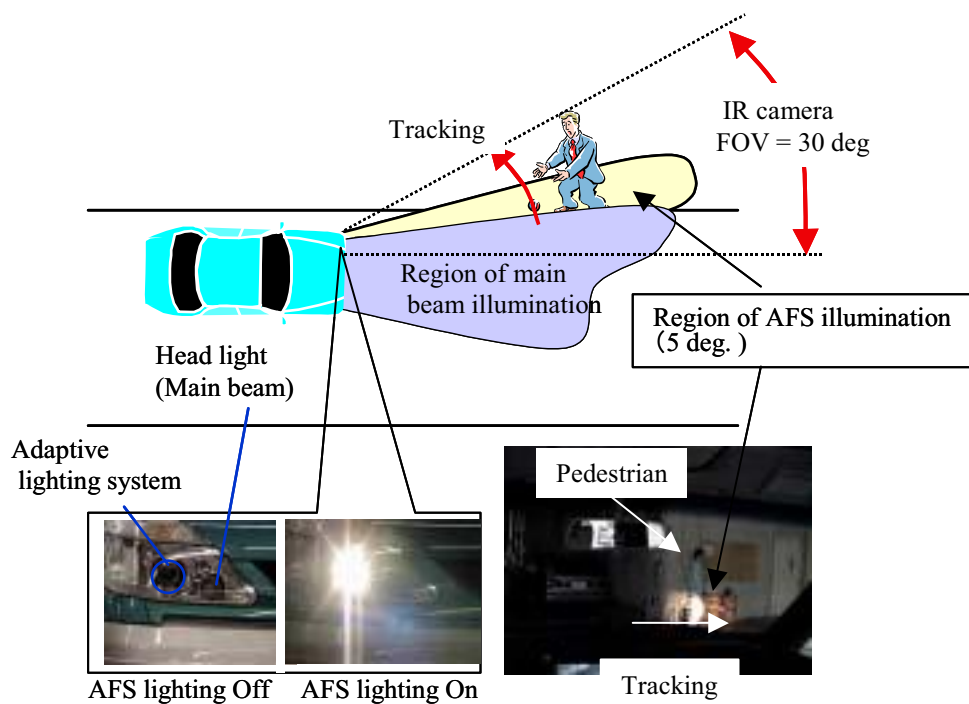
Fig. 14. In-vehicle installation of IR-RC system

Fig. 15. Conceptual diagram of IR-AFS system

4. FUTURE ISSUES

4.1. Overview
This section summarizes various issues that will need to be addressed in order to expand the automotive applications of IR imaging sensors in the future.

4.2 Lower cost
Reducing the IR sensor cost is the biggest issue. Because vehicles themselves are expensive products, there are extremely rigorous demands to reduce the cost of auto parts in general. Uncooled IR imaging sensors are fabricated with micromachining technology, so it takes time to improve the yield, but it is expected that lower-cost sensors will be achieved some day. On the other hand, it will be more difficult to reduce the cost of the 10-μm IR camera because glass cannot be used in its optical system and expensive materials like Ge have to be employed. Though there are some examples of reflective optical systems and the application of plastic lenses, it will be necessary in the future to optimize and reduce the overall cost through (1) optimization of the system design and (2) the use of high-responsivity sensors combined with low-cost lenses. The first important step in that direction is to reduce the sensor cost.

4.3. Higher reliability
For systems that simply provide IR images, it is sufficient to ensure the reliability of the sensors and cameras. However, for a pedestrian detection system and other applications that require a judgment process, it is necessary to improve the reliability of the entire system, which means reducing the risk of non-detection and false detection.

4.4. HMI
Useful information must be provided to drivers without interfering with driving operations and that is not easy to accomplish. Conceivable methods of presenting information include visual and audible means, among others. More effective presentation methods will surely be devised in the future as a result of further progress in ergonomics, IT and display technologies.

4.5. Optical system grime and breakage
These are problems that cannot be avoided on vehicles inasmuch as they travel at high speed in the open air. Moreover, in addition to limits on the range of usable materials, there are also strict demands for lower costs. The issue of road grime will likely require measures similar to the self-diagnostic function of laser radar units.

4.6. Constraints related to installation locations
There are extremely severe constraints on the size and shape of IR sensor units owing to the critical importance of a vehicle's exterior styling and interior design in customers' purchase decisions as well as to the limitations on available cabin space. It will be necessary to downsize sensors further, reduce the diameter of the lens barrel and achieve quieter operation in the passenger compartment, among other improvements

5. CONCLUSION

Infrared sensors are very promising as human body detection devices in systems for improving vehicle safety and occupant comfort, but their high cost has previously prevented widespread automotive use. Completely new approaches have been needed to attain substantial cost reductions. At Nissan, we have developed a new sensor structure and manufacturing process that facilitate the fabrication of low-cost sensors having several thousand to several tens of thousands of elements. As a result, it is now possible for the first time to achieve far-infrared imaging sensors capable of being used widely in automotive and consumer applications.

We have developed a vehicle start-off control system using IR imaging sensors for human body detection around the vehicle and a system for detecting human bodies in the driver's blind spots based on the fusion of a visible camera with IR imaging sensors. Tests conducted with an experimental vehicle have verified the effectiveness of these new systems, which are the first of their kind anywhere in the world in the area of IR sensor systems for automotive application. Moreover, we have also proposed concepts for an IR pedestrian detection system that operates in tandem with an adaptive front lighting system and a hand command system that can recognize the number of extended fingers.

It is hoped that the fusion of IR cameras with other remote sensing systems will lead to the development of easy-to-use sensors having high reliability.

REFERENCES

1. C. Hanson, "Uncooled thermal imaging at Texas Instruments", *SPIE*, Vol. 1689, pp. 330-339, 1993.
2. R. A. Wood, C. J. Han, and P. W. Kruse, "Integrated uncooled IR detector imaging arrays", *Proceedings of the IEEE Solid State Sensor and Actuator Workshop*, pp. 132-135, 1992
3. S. Klapper, R. Kyle, R. Nicklin and A. Kormos, "Night Vision – Changing the Way We Drive", *SPIE*, Vol.4360, pp. 117-121.
4. A. W. Herwaarden and P. M. Sarro, "Thermal sensors based on the Seebeck effect", *Sensors and Actuators A*, Vol. 10, pp. 321-346, 1986.
5. R. Lenggenhanger, H. Baltes, and T. Elbel, "Thermoelectric infrared sensors in CMOS technology", *Sensors and Actuators A*, Vol. 37-38, pp. 216-220, 1993.
6. T. Kanno and M. Saga, "Uncooled infrared focal plane array having 128 x 128 thermopile detector elements", *SPIE*, Vol. 2269, 1994.
7. D. Roger, "Reliable, high quality infrared sensors have found their way into automotive climate control", , *Advanced Microsystems for Automotive Applications 2003*, Springer Verlag, ISBN 3-540-00597-8, pp. 359-376, 2003.
8. E. Mottin, JL. Martin, JL. Ouvrier-buffet, M. Vilain, A. Bain, JJ. Yon, JL. Tissot, " Enhanced amorphous silicon technology for 320x240 microbolometer arrays with a pitch of 35µm", *SPIE*, Vol. 4369, pp. 250-256, 2001.
9. T. Ishikawa, M. Ueno, K. Endo, Y. Nakaki, H. Hata, T. Sone, M. Kimata, T. Ozeki, "Low-cost 320 x 240 uncooled IRFPA using conventional silicon IC process", *SPIE*, Vol.3698, pp.556-564, 1999.
10. M. Hirota, M. Saito, S. Morita, and H. Fukuhara, "Nighttime Pedestrian Monitoring System and Thermal Infrared Technology"*, Jidosha Gijutsu*, Vol. 50, No. 11, pp. 58-63, November 1996 (in Japanese).
11. JJ.Yon, E. Mottin, L. Biancardini, L. Letellier, and JL. Tissot; "Infrared Microbolometer Sensors and Their Application in Automotive Safety", *Advanced Microsystems for Automotive Applications 2003*, Springer Verlag, ISBN 3-540-00597-8, pp 137-157, 2003.
12. M. Hirota, F. Satou, M. Saito, Y. Kishi, Y. Nakajima, and M. Uchiyama, "Thermoelectric infrared imager and automotive applications"*, SPIE*, Vol.4369, pp.312-321, 2001.